PHYSICAL REVIEW B VOLUME 1, NUMBER 6 15 MARCH 1970

Structural, Optical, and Electrical Properties of Amorphous Silicon Films*

M. H. BRODSKY, R. S. TITLE, K. WEISER, AND G. D. PETTIT
IBM Thomas J. Watson Research Center, Yorktown Heights, New York 10598
(Received 6 November 1969)

We report measurements on the x-ray diffraction, electron spin resonance (ESR), optical absorption, and electrical conductivity of amorphous Si films. The x-ray diffraction results show there is no long-range ordering of the atoms in amorphous Si independent of the sample's thermal history, while all of the other properties show strong dependences on annealing. The ESR results indicate a large number of microscopic surfaces distributed throughout the amorphous bulk, and lead us to interpret the optical and electrical properties in terms of "building blocks" with linear dimensions between 10 and 15 Å.

I. INTRODUCTION

AMORPHOUS silicon and germanium have been the subjects of many recent investigations on disordered systems. The amorphous forms of these elemental semiconductors are chosen because of the thoroughly characterized and relatively well-understood crystalline properties. With this extensive background of knowledge about the crystals, one can then study the effects of structural disorder. One objective of such studies is to establish what, if any, features of the conventional band-structure picture of semiconductors are retained in the amorphous state. Clark,[1] Tauc,[2] Grigorovici,[3] Chittick *et al.*,[4] and Walley[5] have recently published surveys on various aspects of the electrical and optical properties of amorphous Si and Ge. A related study on amorphous SiC has been reported by Mogab and Kingery.[6] The above studies have shown that it is difficult to define uniquely the properties of these amorphous materials. For example, the electrical resistivities vary with time and annealing histories. Such effects make it difficult to compare results from different laboratories. Even if allowance for annealing is made, inconsistencies between laboratories are abundant in the literature. Chittick *et al.*[4] report initial resistivities of amorphous Si as much as ten orders of magnitude higher than the films grown by Walley[5] and Tauc.[2] Donovan *et al.*[7] observe a sharp, well-defined optical-absorption edge in amorphous Ge, while Glass,[8] Tauc *et al.*,[9] Grigorovici and Vancu,[10] and Clark[1] report exponential tailing off of the absorption constant at low photon energies. Grigorovici[3] has discussed some additional problems concerning the extrinsic-versus-intrinsic nature of the electric and thermoelectric behavior of amorphous Si and Ge. The structure of amorphous Si and Ge, as well as amorphous solids in general, is also an unresolved point in the literature. X-ray analyses have led to controversies with respect to the ability to differentiate between microcrystalline and continuous network models.[11] For Si or Ge, Coleman and Thomas[12] and Grigorovici and Mănăilă[13] have proposed interconnected substructures of pentagonal duodecahedra. Breitling[14] proposes layered substructures, while Light and Wagner[15] favor microcrystallites. All of these models are based on similar x-ray diffraction data. Recently Brodsky and Title[16] have presented evidence from electron spin resonance (ESR) for the existence of internal surfaces in amorphous Si, Ge, and SiC. Moss and Graczyk[17] corroborate this aspect of the ESR interpretation with their observation of small-angle electron scattering from voids in amorphous Si films.

We have undertaken an experimental survey of the structural, optical, and electrical properties of amorphous Si. Specifically, we address ourselves to the questions of microcrystallinity, uniqueness of the amorphous form, dependence of the properties on thermal history, and the relation of the various properties to each other and to the single crystal properties. The strategy of the study has been to make a series of measurements on the same sample before and after isochronal anneals at increasing temperatures in order to ensure significant comparison between the different results. Our studies consisted of structural examinations by x-ray diffraction and ESR, optical-absorption and index-of-refraction measurements, and room-temperature electrical-conductivity data, all as a function of isochronal

---

* Preliminary oral reports on this study were presented at the March 1969 meeting of the American Physical Society [Bull. Am. Phys. Soc. 14, 311 (1969)], and at the September 1969 International Conference on Amorphous and Liquid Semiconductors in Cambridge, England.

[1] A. H. Clark, Phys. Rev. **154**, 750 (1967).
[2] J. Tauc, Mater. Res. Bull. **3**, 37 (1968).
[3] R. Grigorovici, Mater. Res. Bull. **3**, 13 (1968).
[4] R. C. Chittick, J. H. Alexander, and H. F. Sterling, J. Electrochem. Soc. **116**, 77 (1969).
[5] P. A. Walley, Thin Solid Films **2**, 327 (1968).
[6] C. J. Mogab and W. D. Kingery, J. Appl. Phys. **39**, 3640 (1968).
[7] T. M. Donovan, W. E. Spicer, and J. M. Bennett, Phys. Rev. Letters **22**, 1058 (1969).
[8] A. M. Glass, Can. J. Phys. **43**, 1068 (1965).
[9] J. Tauc, R. Grigorovici, and A. Vancu, Phys. Status Solidi **15**, 627 (1966).
[10] R. Grigorovici and A. Vancu, Thin Solid Films **2**, 105 (1968).
[11] A. Bienenstock and B. G. Bagley, J. Appl. Phys. **37**, 4840 (1966).
[12] M. V. Coleman and D. J. D. Thomas, Phys. Status Solidi **24**, K111 (1967).
[13] R. Grigorovici and R. Mănăilă, Thin Solid Films **1**, 343 (1967).
[14] G. Breitling, J. Vacuum Sci. Technol. **6**, 628 (1969).
[15] T. B. Light and C. N. J. Wagner, J. Appl. Cryst. **1**, 199 (1968).
[16] M. H. Brodsky and R. S. Title, Phys. Rev. Letters **23**, 581 (1969).
[17] S. C. Moss and J. F. Graczyk, Phys. Rev. Letters **23**, 1167 (1969).

annealing. Further experiments were performed on other samples to determine how sensitive the general trend of the results was to ambient atmosphere, method of sample preparation, oxygen impurities, possible partial crystallization, and annealing conditions. We have found that in addition to the previously known sensitivity of resistance to annealing, the optical absorption, index of refraction, and number of spins observed in ESR are also significantly dependent upon the thermal history of a given sample. We propose an interpretation of the results in terms of a model of amorphous Si containing a large density of internal microstructure surfaces.

There are some important qualitative differences between the tetrahedrally coordinated amorphous semiconductors such as Si and Ge (and probably SiC, GaAs, etc.) and the "genuine" glassy amorphous semiconductors such as the chalcogenide-based compounds (e.g., As_2Se_3, As_2Te_3). Genuine glasses,[18,19] which can be prepared by quenching of a melt, exhibit glass transition temperatures and have similar structures in their liquid and amorphous solid phases. On the other hand, amorphous Si and Ge cannot be prepared from the melt and are usually obtained by quenching a vapor. Furthermore, the structure of amorphous Si and Ge is latticelike,[14] not liquidlike,[20] as in a glass. That is, solid amorphous Si and Ge preserve the tetrahedral coordination[21,22] of their crystal phases rather than the body-centered coordination of their liquid phases. Gubanov[19] has compared the liquid and amorphous solid electrical properties of Si and Ge with other amorphous semiconductors.

In Sec. II we describe the methods of sample preparation and the experimental techniques. The experimental results are presented and discussed in Sec. III. In Sec. IV we suggest and discuss a model to account for the structural, optical, and electrical observations of amorphous Si films. The results are summarized in Sec. V.

II. EXPERIMENTAL PROCEDURES

The samples used in this study were thin films of Si deposited on substrates of single crystal sapphire, which were held at or below room temperature. The majority of the films was deposited by rf sputtering of a 6-in.-diam intrinsic silicon cathode. The sapphire substrates were 0.010 in. thick and $\frac{3}{4}$ or 1 in. in diameter. During the deposition, thermal contact between the substrate and a water-cooled copper block was made by painting the contact area with gallium. The actual temperature of the film during growth appears to depend on the quality of the thermal contact, the substrate thickness and material, and the duration of the deposition. The sputtering was carried out in an argon atmosphere at a pressure of 0.01 Torr after pre-evacuation of the oil-pumped chamber to 10^{-7} Torr. Deposition rates were in the range between 200 and 600 Å/min. After growth and between measurements, the films were stored in air. The thicknesses of the Si layers varied from 0.3 to 10 μm and were determined to within $\pm 10\%$ by Tallysurf or Tolansky fringe measurements across etched or grown steps in the films.

The films grown in this manner were opaque and had smooth silvery mirror faces. The films were hard, adhered well to the substrates, and could be handled extensively with reasonable care. Such handling included scribing and separating pieces, rinsing in solvents, etching, ultrasonic machining of patterns for resistivity measurements, and depositing and removing contacts or mounting cement.

For each series of measurements described below, four pieces of the same sample were used. After each section of the sample was measured, the four pieces were sealed in a quartz ampoule, evacuated to approximately 10^{-6} Torr, and then isochronally annealed at increasing temperatures between 50 and 950°C. After each anneal the sample was removed from the ampoule for the measurements. The annealing time was generally two hours.

Four types of measurements were made on each sample before and after each anneal. (1) The x-ray diffraction pattern of the Si film was taken in a Debye-Scherrer camera using copper $K\alpha$ radiation incident at a glancing angle. (2) The optical transmission spectrum in the region from 0.5 to 3.0 eV was obtained with a Cary-14 double-beam spectrophotometer. The optical-absorption coefficient α of a film with thickness d was deduced from the transmission T by estimating the reflection losses for the two-layer film-substrate structure according to the following formula[23]:

$$T=\frac{(1-R_1)(1-R_2)(1-R_3)e^{-\alpha d}}{(1-R_2R_3)\{1-[R_1R_2+R_1R_3(1-R_2)^2]e^{-2\alpha d}\}}, \quad (1)$$

where R_1, R_2, and R_3 are the reflectances at the air-film, film-substrate, and substrate-air interfaces, respectively. This approximation includes all the noncoherent multiple reflections. In those spectral regions where coherence was important, i.e., where interference fringes were observed, we approximated T by the average of the maximum and minimum transmission. The order of each interference fringe was identified and used to calculate the index of refraction n from the conditions for maximum and minimum transmissions in regions of small absorptions. The index of refraction at 2 μm was used to calculate R_1 and R_2. (3) The electrical conductivity was measured using standard four-probe techniques on suitable sample geometries ultrasonically machined out of the film. The contacts were made with silver paste and were etched off before annealing. (4)

[18] B. T. Kolomiets, Phys. Status Solidi 7, 359 (1964).
[19] A. I. Gubanov, *Quantum Electron Theory of Amorphous Conductors* (Consultants Bureau, Inc., New York, 1965), Chap. I.
[20] H. Richter, J. Vacuum Sci. Technol. 6, 631 (1969).
[21] H. Richter and O. Fürst, Z. Naturforsch. 6a, 38 (1951).
[22] H. Richter and G. Breitling, Z. Naturforsch. 13a, 988 (1958).
[23] R. Tsu, W. E. Howard, and L. Esaki, Phys. Rev. 172, 779 (1968).

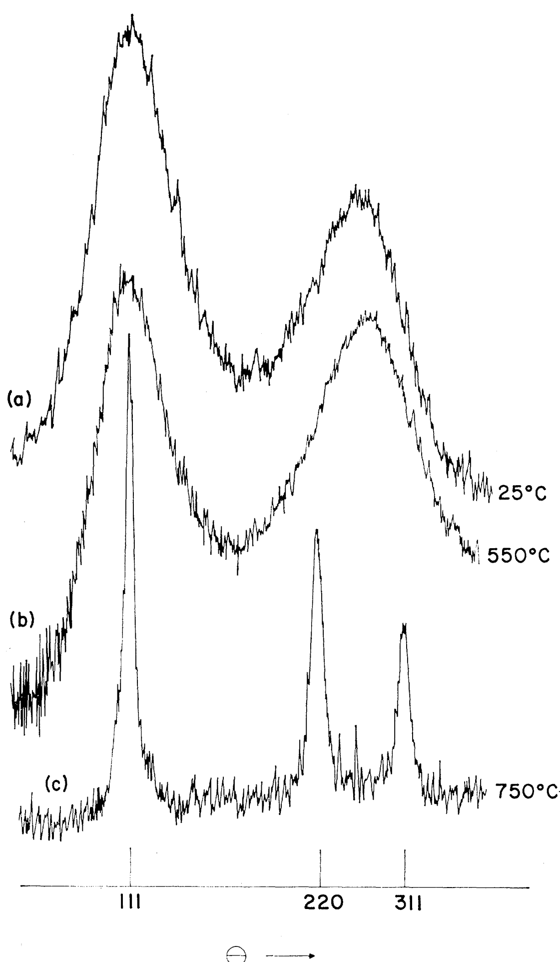

FIG. 1. Normalized microdensitometer traces of x-ray diffraction photographs of a sputtered amorphous Si film after three representative annealing steps. The curves are displaced vertically for clarity. Trace (a) was taken from a picture of a fresh film that had never been raised above room temperature. Trace (b) was taken after the film was annealed three hours each at 62, 100, 175, 250, 325, 400, 475, and 550°C. It indicates that the film was still amorphous and is representative of the traces obtained after each of the eight anneals. Trace (c) is representative of a crystallized film and was taken after the next anneal at 750°C.

The ESR signal was measured at 77°K in an X-band microwave bridge with the sample in a 6-in. magnet. Relative signal strengths were determined by comparison with a stable standard Si sample. We estimate the accuracy of our comparisons to be about $\pm 10\%$, limited by the reproducibility of insertions and cavity tuning. Each comparison was repeated at least once, and the results presented are averages of all comparisons for a given annealing condition. The g factor of the signal was determined from a comparison with a standard of Mn^{2+} in a SrS host. The ESR signals of the Mn^{2+} ions in this material bracket the signal of the Si and therefore are easier to use as a standard than diphenylpicrylhydrazyl (DPPH), whose ESR signal overlaps that of the Si signal. The absolute number of spins was found by comparing the signals of the various thicknesses of Si films with those of a measured amount of DPPH.

Although most of the measurements were performed on sputtered films as described above, part of the study used evaporated films. The evaporations were made in a dry-pumped ultrahigh vacuum system with a base pressure of about 2×10^{-10} Torr in the evaporation chamber. The source material was electron-beam heated and condensed on a liquid-nitrogen cooled substrate. The pressure during evaporation varied between 2×10^{-8} and 5×10^{-7} Torr, depending on the deposition rate. Deposition rates between 75 and 850 Å/min were used. Measurements of the sample resistance were made without breaking the vacuum. Using predeposited electrodes, we monitored the resistance as a function of time and temperature from immediately after growth until the sample was eventually removed from the vacuum. Four-probe and two-probe resistance measurements gave the same results. Occasionally, optical-absorption and ESR data were taken shortly after the films were removed from vacuum. We found essentially the same optical or ESR properties for the evaporated and sputtered films.

For the sake of completeness, we also made some depositions in the manner of Chittick *et al.*[4] by a rf glow discharge decomposition of silane. No detailed measurements were made on these films other than ascertaining that their resistivities were many orders of magnitude higher than those of films condensed from Si vapors, and that they showed a strong optical absorption near 1.7 eV, just as reported in Ref. 4.

III. RESULTS

In this section we present the results of our measurements on the structural, optical, and electrical properties of amorphous Si. Our aim is to present data on the properties themselves and to indicate how the properties are related to the thermal history of the sample and to one another.

First we discuss the x-ray diffraction results and use them to define the amorphous form of Si. Figure 1 shows microdensitometer traces of the x-ray diffraction photographs for a Si film at three representative stages in a series of isochronal anneals. Trace (a) is the pattern obtained when the sample had never been raised above room temperature. Trace (b) is typical of the pattern after each of eight isochronal annealing steps, and was taken after the sample was annealed at 550°C. Trace (c) came after a subsequent anneal at 750°C. The main feature of these x-ray diffraction pictures is that all the patterns of amorphous Si are essentially the same [e.g., traces (a)&(b) for all annealing temperatures below the crystallization temperature]. All subsequent anneals then continue to give patterns like trace (c), which is characteristic of fine-grain polycrystalline Si. The diffraction patterns before crystallization appear as halos on the original photographs. Such patterns of broad

halos are indicative of an amorphous material and have been interpreted[12–14,21,22] in terms of various disordered continuous arrangements of atoms. An alternate interpretation of the same data is that the halos are due to small microcrystallites with the small number of diffraction planes per crystallite resulting in a broadening of the normally sharp line of the powder diffraction pattern.[15] The angular width at half-height of the halo centered near 28.4° is about 8°±1°. In crystalline Si, this peak corresponds to the Bragg reflections from {111} planes. If we use the Scherrer formula,[24] the observed width implies that *if* the material is microcrystalline, the crystallites have linear dimensions of approximately 11 to 15 Å or about two or three unit cells across. It should be emphasized that the "microcrystallites," i.e., building blocks, need not have the same detailed structure[17] as crystalline Si and most likely would not, because of their large surface-to-volume ratio. Because of the ambiguity in the interpretation of the x-ray diffraction data, we shall adopt as a working definition of amorphous Si that it is the phase that is characterized by diffuse halos in a diffraction pattern and present other experimental data to shed more light on the details of the structure of amorphous Si. No gross variations are observed in the character of the x-ray[14,21,22] or electron[17,25] diffraction patterns as a function of increasing temperature until crystallization is reached. We have looked for and not found any x-ray evidence for incipient crystallization during annealing cycles at temperatures below the crystallization temperature. The crystallization temperature is not unique for amorphous Si. Crystallization occurs in the 450–650°C range[22,25,26] and probably depends on sample purity, thickness, environment, and substrate[27]; no comprehensive study of these effects has been reported.

A strong ESR signal was easily detected in amorphous Si at 300, 77, and 4°K.[16] Figure 2 shows the trace of a

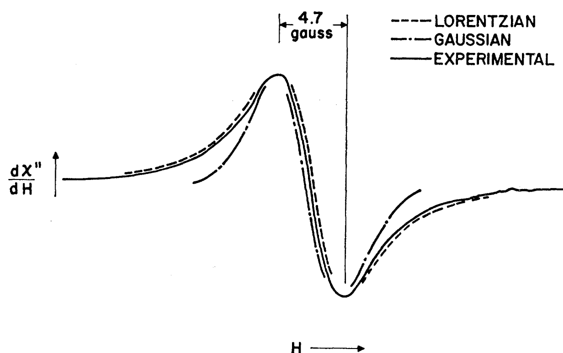

FIG. 2. Typical ESR signal for amorphous Si. Gaussian and Lorentzian line shapes are shown for comparison.

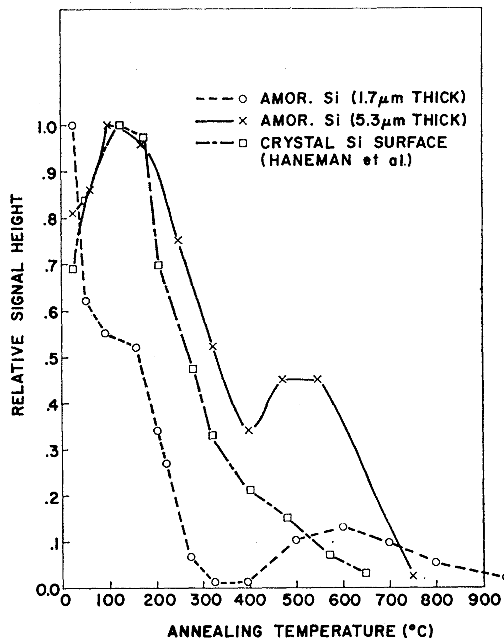

FIG. 3. Comparison of the annealing of the ESR signal strengths for two amorphous Si films and a polished single-crystal Si surface. (See Ref. 31.)

typical magnetic-field sweep at 77°K. At all observation temperatures the g value of the resonance is 2.0055 ±0.0005. The line shape is Lorentzian, with a width of 4.7 G at 9.4 GHz. Ditina *et al.*[28] have reported a similar but wider resonance in evaporated Si films. This laboratory[16] has already reported on ESR in amorphous Si; in contrast with the interpretation of Ditina *et al.*,[28] the resonances were identified as arising from the same kind of electronic states responsible for the ESR observations of the surface region of single-crystal Si.[29] The signals we observed arose from throughout the bulk of the amorphous Si, as evidenced by the constant spin density of 2×10^{20} spins/cm^3 found in room-temperature annealed films of varying thicknesses.[16] Using Haneman's[29] estimate of one spin per ten {111} surface atoms on freshly cleaved room-temperature single-crystal Si, we deduce of order 2×10^{21} (surface atoms)/cm^3 in amorphous Si. It is well known that low-energy electron-diffraction (LEED) examination of the {111} surfaces of cleaved Si single crystals shows a characteristic two-dimensional structure,[30] which undergoes a cleaved-to-annealed transformation[30] at about 600°C to a new arrangement. Haneman and co-workers[29,31] have identified the surface spin resonance and its annealing be-

[24] See, for example, L. Azároff, *Elements of X-Ray Crystallography* (McGraw-Hill Book Co., New York, 1968), Chap. 20.
[25] J. F. Graczyk, Ph.D. thesis, M.I.T., 1968 (unpublished).
[26] J. C. Evans, Jr., NASA Technical Note No. D-4522, 1968 (unpublished).
[27] R. F. Adamsky, K. H. Behrndt, and W. T. Brogan, J. Vacuum Sci. Technol. **6**, 542 (1969).
[28] Z. Z. Ditina, L. P. Strakhov, and H. H. Helms, Fiz. Tekh. Poluprov. **2**, 1199 (1968) [English transl.: Soviet Phys.—Semicond. **2**, 1006 (1969)].
[29] D. Haneman, Phys. Rev. **170**, 705 (1968).
[30] J. J. Lander, G. W. Gobeli, and J. Marrison, J. Appl. Phys. **34**, 2298 (1963).
[31] D. Haneman, M. F. Chung, and A. Taloni, Phys. Rev. **170**, 719 (1968); G. K. Walters and T. L. Estle, J. Appl. Phys. **32**, 1854 (1961).

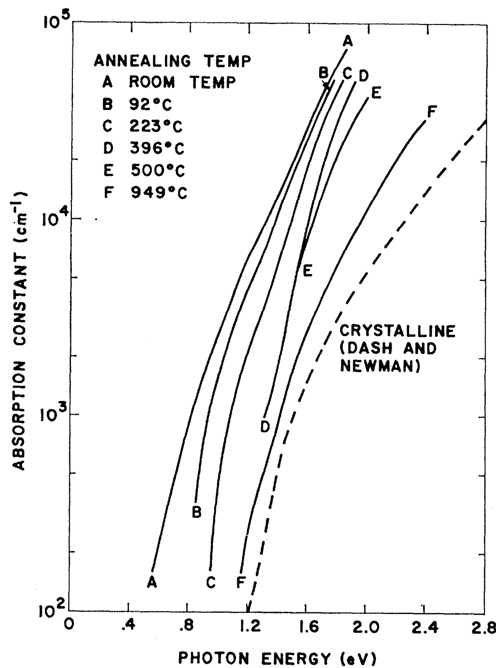

FIG. 4. Room-temperature optical-absorption constant versus photon energy for a film annealed for about two hours at 25, 52, 92, 160, 204, 223, 275, 396, 500, 601, 700, 800, and 949°C. For clarity, only spectra after six of the anneals are shown. This sample crystallized during the 500°C annealing cycle. The dashed line is from the single-crystal Si spectrum reported by Dash and Newman. (See Ref. 32.)

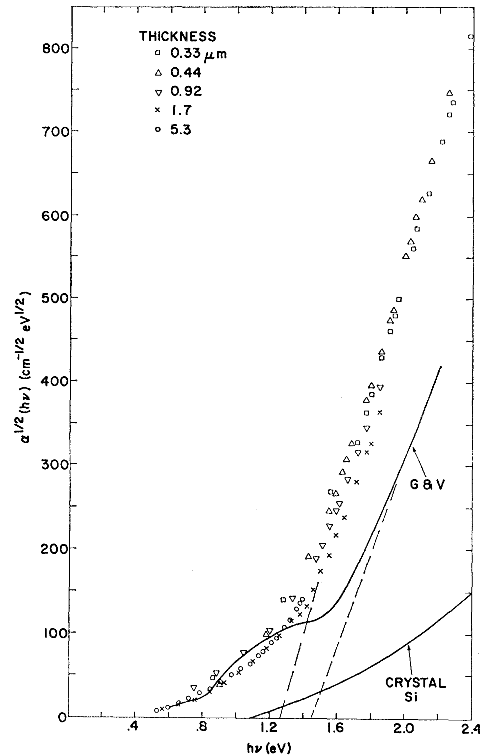

FIG. 5. Room-temperature optical-absorption spectra for five films plotted to illustrate the dependence of $(\alpha h\nu)^{1/2}$ on $h\nu$. The line labeled G and V is the spectrum for amorphous Si reported by Grigorovici and Vancu (Ref. 10). The solid line is the spectrum for single-crystal Si reported by Dash and Newman (Ref. 32).

havior with the surface structure and transformation observed by LEED. In Fig. 3 we compare the annealing of the amorphous Si ESR signal strength with the annealing of the surface ESR on single-crystal Si. The similarity of the results indicates a correlation between the annealing of the crystal surface and of the amorphous bulk. The small rise in signal strength from the films after crystallization may be due to cracking during cooling of the newly formed crystals. Mechanical damage, such as cracking and polishing, has been shown to result in increased surface areas and stronger ESR signals of the same g value, linewidth, and shape.[31] We observe no changes in g value, linewidth, or line shape as a function of annealing history.

Figure 4 shows the room-temperature optical-absorption spectra for amorphous silicon films after representative stages in the annealing procedure. This particular sample was annealed in steps of about 50–100°C and crystallized during the 500°C annealing cycle. The absorption spectra, like the ESR signal strength and electrical conductivity, is seen to be strongly dependent on the sample's thermal history. Also shown for reference is the absorption spectrum of single-crystal silicon reported by Dash and Newman.[32] The data on our crystallized films agree in shape and approximate magnitude with the single-crystal absorption spectrum. We have tried to fit appropriate parts of the spectra for amorphous Si to relations of the form

$$\alpha \propto (h\nu - E_G)^2/nh\nu \tag{2}$$

or

$$\alpha \propto e^{h\nu/E_0}, \tag{3}$$

where $h\nu$ is the energy of the photons, and E_G or E_0 could be interpreted as characteristic energies of the

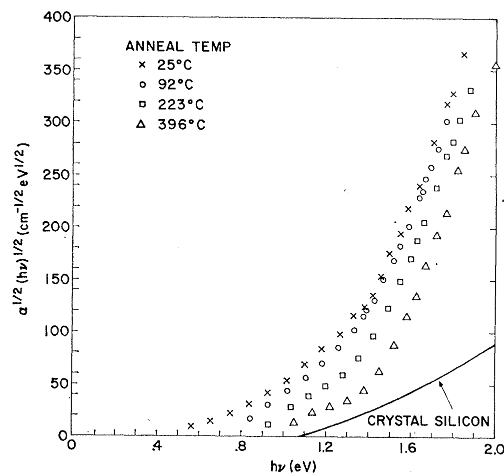

FIG. 6. Room-temperature optical-absorption spectra of amorphous Si plotted as $(\alpha h\nu)^{1/2}$ against $h\nu$ for four different annealing temperatures. The annealing conditions are given in the caption of Fig. 4.

[32] W. C. Dash and R. Newman, Phys. Rev. 99, 1151 (1955).

distribution of electronic states in bandlike and tail-like regions, respectively. Absorption data on glassy chalcogenide semiconductors have been fitted to Eq. (2) at high-absorption constants[33,34] ($>10^4$ cm^{-1}) and to Eq. (3) at lower-absorption constants.[34,35] Such fits are interpreted in terms of a model with parabolic densities of states for energies well away from a hypothetical pseudogap and with a disorder-induced tailing off of states into the pseudogap.[33–37]

Figure 5 shows a plot of $(\alpha h\nu)^{1/2}$ against $h\nu$ for Si films of five different thicknesses. Although all five films were sputtered under the same conditions onto substrates nominally held at room temperature or below, the films apparently underwent some heating during the sputtering process, and therefore the thicker films show some annealing effects even in this as-grown condition. Equation (2) appears to give a reasonable fit to the data of the higher-absorption region; however, one must be careful about the meaning of such fits for such a limited range of data. It is not unreasonable to neglect the small n dependence in such a plot, but any detailed interpretation should include the n dependence and the dependence of the optical-transition matrix elements on energy.[38] For the approximation of constant matrix elements, Eq. (2) is expected to hold when all transitions are allowed between energy regions each having a parabolic density of states. Grigorovici and Vancu[10] found a straight-line fit of $(n\alpha h\nu)^{1/2}$ versus $h\nu$ for $h\nu$ between 1.9 and 2.3 eV. Figure 5 shows that our data for $(\alpha h\nu)^{1/2}$ versus $h\nu$ give an E_G of 1.26 eV, compared with Grigorovici and Vancu's threshold of 1.44 eV. We believe the difference can be attributed to different annealing histories. Although Grigorovici and Vancu do not specify the thermal histories of their samples, we surmise from our annealing data that they used films annealed at temperatures just short of crystallization. The effect of annealing is shown in Fig. 6. We see that the spectra and the extrapolated thresholds depend on thermal history, with the highert-hreshold energies occurring after the higher-temperature anneals. For all annealing temperatures observed, the threshold energy E_G was larger than the optical band gap of single-crystal Si.[39]

In the lower-absorption region there is a tailing of the absorption spectrum, but the tailing is not strictly exponential (see Fig. 4). We do not see the structure reported in the tail by Grigorovici and Vancu.[10]

It is important to note two physically significant features of the absorption spectra of amorphous Si relative to crystalline Si. First, the absorption constants are considerably higher throughout the observed spectral range and second, there is a strong absorption tail at energies well below the crystalline band gap. The latter effect is more prevalent in unannealed samples but is still clearly apparent after all anneals which leave the films uncrystallized.

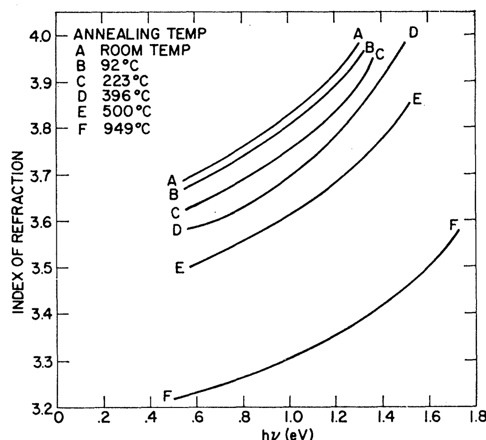

FIG. 7. Room-temperature index of refraction versus photon energy for the same film and annealing conditions as in Fig. 4.

Figure 7 shows the room-temperature index of refraction n versus photon energy for the same sample whose absorption spectra are shown in Fig. 4. The crystallized-film data agree with the literature[40] values within the estimated 10% uncertainty due to the measurement of film thickness. In Fig. 8 we plot the dependence of the room-temperature index of refraction at 2 μm on the isochronal annealing temperature. The break in the slope of the straight lines drawn through the data points coincides wlth the onset of crystallization as observed by x-ray diffraction.

In Fig. 9 we compare the annealing of the ESR, optical, and electrical properties of a sample as characterized by the ESR signal strength, the index of refraction at 2 μm, and the electrical conductivity. The

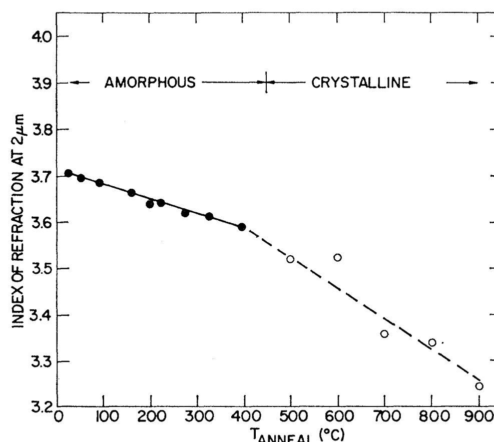

FIG. 8. Room-temperature index of refraction at 2 μm versus annealing temperature for the same film and conditions as in Fig. 4.

[33] K. Weiser and M. H. Brodsky, Phys. Rev. **B1**, 791 (1970).
[34] W. E. Howard and R. Tsu, Phys. Rev. B (to be published).
[35] J. T. Edmond, Brit. J. Appl. Phys. **17**, 979 (1966).
[36] N. F. Mott, Advan. Phys. **16**, 49 (1967).
[37] M. Cohen, H. Fritsche, and S. Ovshinsky, Phys. Rev. Letters **22**, 1065 (1969).
[38] See, for example, R. A. Smith, *Semiconductors* (Cambridge University Press, London, 1959), Chap. 7.
[39] G. G. MacFarlane, T. P. McLean, J. E. Quarrington, and V. Roberts, Phys. Rev. **111**, 1245 (1958).
[40] C. D. Salberg and J. J. Villa, J. Opt. Soc. Am. **47**, 244 (1957).

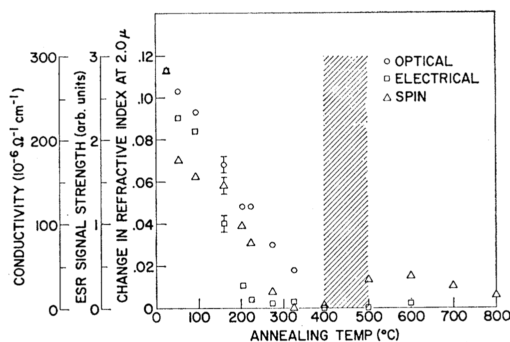

FIG. 9. Dependence on annealing temperature of the room-temperature electrical conductivity, strength of ESR signal, and change in refractive index. The shaded area separates the amorphous from polycrystalline regions.

ESR signal strength is a measure of the number of electrons with unpaired spins distributed on surfaces throughout the sample. The index of refraction is proportional to the number of states contributing to the optical absorption and the transition probabilities between them. The electrical conductivity reflects not only changes in the number of states available for the conduction processes, but also changes in mobility and activation energy. All three of these properties decrease in magnitude as a function of annealing temperature. This behavior is to be compared with the relative insensitivity of the structure as determined by concurrent x-ray diffraction observations. The annealing points to a correlation of electrical conductivity and optical absorption with the number of unpaired electrons.

Before we continue with the discussion, it appears proper at this point to consider the validity of interpreting the above results in terms of "true" annealing, i.e., structural changes in the bulk, particularly in the light of the past and present discrepancies in the literature on amorphous Si and Ge. We have considered three possible sources of systematic errors that might give spurious annealing trends and have decided, by the arguments given below, that the observed effects are real structural changes, intrinsic to the annealing of amorphous Si. The possible spurious effects we considered are the following: cracking of the films due to thermal stresses between film and substrate, oxygen contamination from the ambient atmosphere either during annealing or measurement, and incipient partial crystallization of the films.

Microscopic cracking of the films might be expected to occur due to stresses resulting from a thermal-expansion mismatch at the film-substrate interface. Such cracking during each annealing cycle could conceivably result in voids, and therefore the optical absorption coefficient and electrical conductivity would appear to decrease after each anneal. However, such cracking would result in more Si surface area and give an increase (as is seen on mechanically damaged crystal surfaces[31,32]) rather than a decrease in the ESR signal intensity.

We eliminate the possibility that oxygen contamination, particularly during the annealing stages of each cycle, is responsible for the observed effects because of the following observations: (1) The infrared absorption of the Si-O vibration near 9 μm has been looked for and not seen. For this search we used amorphous Si films grown on single-crystal Ge substrates which were transparent in the 9-μm spectral range. On the basis of the absorption strength of the Si-O vibrations,[41] we estimate the sensitivity to have been enough to detect an oxygen concentration of 10^{16} cm^{-3}. (2) We have examined the annealing behavior of the conductivity of amorphous Si evaporated and measured in ultrahigh vacuum (i.e., pressures less than 10^{-9} Torr) and have found essentially the same qualitative behavior reported by others at higher pressures and essentially the same results obtained by our annealing in evacuated quartz ampoules. At such low pressures there is less than a monolayer of oxygen incident on the Si film during an annealing cycle. When O_2 was later admitted into the vacuum system, the conductivity fell by about 15%, which is insignificant compared to the annealing effects, which typically involve orders-of-magnitude changes. Figure 10 shows the resistivity versus temperature and the temperature history for such an ultrahigh vacuum-evaporated and measured amorphous Si film. (3) Annealing the sputtered amorphous Si in flowing H_2 or forming gas (10% H_2, 90% N_2) for two hours at 350°C was qualitatively equivalent to annealing the film sealed in quartz ampoules. Approximately (within ±20%) the same decreases in ESR signal strength, optical-absorption coefficient, and electrical conductivity were observed.

The most bothersome possibility for a spurious effect is the case of incipient crystallization of some of the Si in the amorphous film. Such partial crystallizations have been observed in amorphous Ge films.[42] If more of the film crystallized during each annealing cycle, then we would expect a continuous variation in the measurements between the limits of "pure amorphous" and totally crystalline Si. We have already mentioned that no signs of such incipient crystallites were observed in our x-ray diffraction patterns. The sensitivity is such, however, that at least 10% of the film would have to be crystalline to be observable above the amorphous background. The annealing effects observed are so large that even as much as 10% crystallization of the sample could not be responsible for the observations. Further evidence is indicated by the straight lines in Fig. 8, indicating a break in the index of refraction–versus–annealing-temperature data at the crystallization temperature. We believe that the annealing effects above the crystallization temperature are due to an increasing amount of crystallization and increasing crystalline grain size.

[41] W. Kaiser and P. H. Keck, J. Appl. Phys. 28, 882 (1957).
[42] A. Barna, P. B. Barna, E. F. Pócza, N. Croitoru, A. Dévényi, and R. Grigorovici, Proc. Colloq. Thin Films, Budapest, 1965 (unpublished).

IV. INTERPRETATION OF RESULTS

The results of measurements on amorphous Si can be divided into two groups. First, our own and previous investigations establish it as a semiconductor of lower electrical conductivity than crystalline Si and with a stronger optical absorption in the vicinity of the fundamental absorption edge. Also, we observe a large number of unpaired crystal-surface-like electrons distributed throughout the bulk of amorphous Si. We also reaffirm that there is no long-range ordering of the atoms in amorphous Si. Second, we find that all of these properties except the lack of long-range order depend strongly on the thermal history of the particular sample under study. Thus we want a model, or at least a point of view, for amorphous Si that can account for the observed parameters, their annealing behavior, and their interrelation.

Starting with the structural results of the x-ray and ESR measurements, we propose that one useful picture of amorphous Si is that it consists of an aggregate of "building blocks" with linear dimensions roughly in the 10–15 Å range. These submicroscopic structures are to be distinguished from conventional crystallites in polycrystalline material by the fact that their size does not increase beyond 15 Å upon annealing. The microstructures could be the "amorphons" suggested as the name[13] for the pentagonal duodecahedra postulated by Grigorovici and Mănăilă[13] and by Coleman and Thomas.[12] The maximum-size estimate comes from the widths of the diffraction halos indicating no long-range order, while the lower limit is a consequence of the narrow Lorentzian linewidth of the ESR signal. We identified the signal as arising from surface states, which implies dimensions of at least several atoms. Furthermore, a narrow Lorentzian resonance line almost certainly arises from exchange or motional narrowing,[43] which means the unpaired electron at the surface ("dangling bond") must be sampling the environment of several sites; that is, it hops back and forth between equivalent adjacent surface atoms.

The ESR observation of surfaces implies the existence of voids between the building blocks. Indeed, Moss and Graczyk[17] interpret their observation of small-angle electron scattering in amorphous Si in terms of voids or pores. The presence of voids is also consistent with a model of a continuously disordered network. The principal conceptual difference between building blocks and the continuous network models is the sharp discontinuities between microstructures, which would not be present in the latter model. Some evidence for these discontinuities in the form of barriers to electrical conductivity will be discussed below.

The x rays show only small, if any, changes with annealing; this means that the number and size of the microstructures are not changing, but only that more

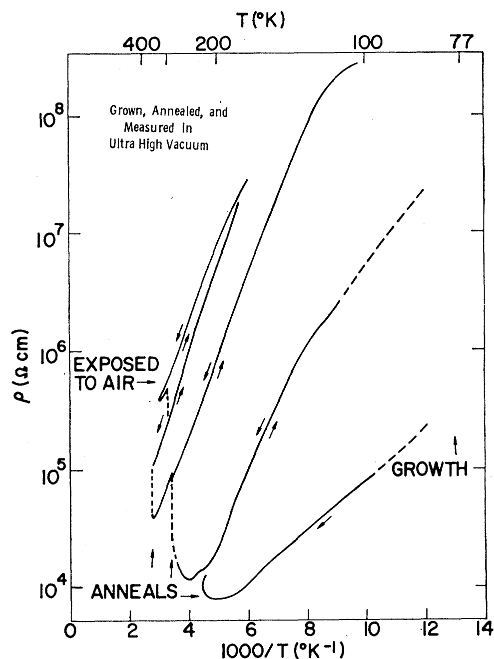

FIG. 10. Resistivity versus reciprocal temperature of an evaporated amorphous Si film grown and measured in ultrahigh vacuum. The subsequent admitting of air is seen to give a small effect compared to annealing effects.

subtle atomic and electronic rearrangements are taking place during precrystallization anneals. Moss and Graczyk's[17] electron-diffraction results on Si, as well as x-ray diffraction measurements of Ge,[14] do reveal a slight narrowing of the halos with annealing. The small changes are consistent with the observations of Longini and Pansino[44] on amorphous Ge of small annealing activation energies (~0.1 eV). Mogab and Kingery[6] deduced somewhat higher (~0.4 to 2.3 eV) activation energies for SiC annealing. We would expect those of Si to be somewhere between these.

We can interpret the amorphous-to-crystalline Si transition in terms of the LEED observations[30] of a cleaved-to-annealed transition on single-crystal Si surfaces near 600°C. In this temperature range the mobilities of the surface atoms of the microstructures are high enough for significant atom movements, resulting in the growth of the more conventional larger-grain polycrystalline Si. Both the Ge cleaved-to-annealed surface transformation[30] and the corresponding amorphous-to-polycrystalline change[22,42] in the films occur at lower temperatures (200–400°C).

The existence of a large number of microscopic surfaces means that an optical-absorption measurement is sampling a material with a large fraction of the atoms on or adjacent to a surface layer. Thus the optical properties of amorphous Si should reveal surface effects not normally observable in crystalline Si because of the

[43] P. W. Anderson and P. R. Weiss, Rev. Mod. Phys. **23**, 269 (1953).

[44] R. L. Longini and S. R. Pansino, J. Appl. Phys. **40**, 2653 (1969).

much larger ratio of surface to volume in the amorphous Si. In the surface region, which contains a large number of "dangling bonds," the bulk crystalline electronic bonds are distorted and shifted by local strains and the electric fields. The strains may be small a few atoms away from the surface, but in the surface layer shifts as large as 0.1 Å in interatomic spacing have been deduced[29] from LEED observations. This is a huge strain (of order of 5%) and is not ordinarily obtainable in the usual kind of hydrostatic pressure or uniaxal stress experiment. Nevertheless, for the purposes of a rough estimate, we extrapolate the hydrostatic data,[45] which indicates a change in optical band gap of about -7 eV per unit strain. The large strains in the surface region should lead to tailing and result in a decrease of about 0.4 eV in the onset of the observed optical absorption. In addition to strains, the surface region of crystal Si can have large electric fields due to band bending induced by the charged "dangling bonds" and other surface states. Redfield[46] has tried to account for the optical-absorption tails in GaAs using the Franz-Keldysh effect of the electric fields associated with localized states. Similar electric-field effects may be occurring in amorphous Si in addition to the strains. Fischer[47] has speculated that these fields may be as important as strain to the tailing of the optical-absorption edge of irradiated Si. Heavily damaged Si, as occurs in ion-bombarded crystals, is very similar to amorphous Si in its ESR and optical properties.[48]

In the spectral regions just above the respective fundamental absorption thresholds (see Fig. 5), the crystalline-Si absorption constants are much smaller than those of amorphous Si. The relative weakness of the crystal-Si absorption is due to the crystal-momentum selection rule requiring phonon-assisted processes for transitions from the top of the valence band at the center of the Brillouin zone to the bottom of the conduction band near the [100] zone edge. In amorphous Si, a relaxation[2,3,9,10] of this selection rule is expected because of the lack of long-range order due to the finite microstructural sizes and the surface asymmetries. If the band structure is essentially preserved in the amorphous state, i.e., the conduction band minimum is still located at the same position in the Brillouin zone, then one would expect this relaxation of the selection rules to lead to a great increase in the optical absorption near the crystalline energy gap. Fletcher[49] points out, however, that one should expect that the Γ-point sections of the band structure are those most likely to be retained in an amorphous solid with the same short-range correlations as in its crystal form.[50] These short-range angular correlations exist in amorphous Si. If we accept Fletcher's interpretation and attribute the strong optical absorption to transitions between Γ-like band structure remnants, then the energy separation involved would have to be much less than the several electron volt direct gap in crystal Si. The optical-absorption data alone do not allow us to distinguish between the above possibilities, but some support for this point of view comes from recent electroreflectance data by Piller *et al.*,[51] which indicates that the Γ transitions are preserved in amorphous Ge with a decrease in the energy separations.

The decrease in the optical-absorption constant in the tail and the shift of the tail to higher energies with annealing could be attributed to the decrease in strains and fields that accompany the annealing of the submicroscopic surfaces. However, it is noted that the optical-absorption constant at higher energies still remains much higher than that of crystalline Si as long as the films are amorphous. The strength of the fundamental optical absorption is not appreciably affected although the extrapolated threshold shifts to higher energies with annealing.

It is now necessary to consider the electrical data and possible reasons for the low conductivity of amorphous Si and the further reduction of the conductivity with annealing. In considering the effects of annealing on the electrical conductivity, one first notes the correlation between the fall in conductivity and the number of unpaired electrons (Fig. 9), i.e., the "dangling bonds." This fall in conductivity with number of unpaired electrons is consistent with the concept of voids acting as electrically active centers that provide the carriers. For such an interpretation the voids could be either between microstructures or embedded in a continuous network. However, the observed increase in activation energies[3] with annealing indicates that the conductivity decreases cannot be attributed just to a decrease in the number of electrically active centers. In terms of the microcrystallite point of view, it appears that the "dangling bonds" enhance the transfer of carriers between microcrystallites. Supporting evidence for this structural interpretation can be found, in our opinion, in the observations of Walley[5] and Grigorovici *et al.*[3] These authors report an exponential current-voltage relation of a form, which, we believe, indicates that internal barriers (such as might occur between microcrystallites) are limiting the conductivity.

Finally, we make a few remarks comparing the results on sputtered amorphous Si films to other studies. As already pointed out, the results of measurements on the electrical and optical properties of amorphous Si films

[45] See, for example, W. Paul, J. Phys. Chem. Solids **8**, 196 (1959).
[46] D. Redfield, Phys. Rev. **140**, A2056 (1965).
[47] J. E. Fischer, Phys. Rev. **181**, 1368 (1969).
[48] B. L. Crowder, R. S. Title, M. H. Brodsky, and G. D. Pettit, Appl. Phys. Letters **16** (1970).
[49] N. H. Fletcher, Proc. Phys. Soc. (London) **91**, 724 (1967).
[50] J. Stuke [in Proceedings of the International Conference on Amorphous and Liquid Semiconductors, Cambridge, 1969, (unpublished)] has a different interpretation of the role of the short-range angular correlations, which emphasizes the importance of the ⟨111⟩ binding directions.
[51] H. Piller, B. O. Seraphin, K. Markel, and J. E. Fischer, Phys. Rev. Letters **23**, 775 (1969).

either evaporated or sputtered are consistent with each other but do not agree with the corresponding data taken on amorphous Si prepared by the rf decomposition of silane.[4] Detailed x-ray analysis of the silane-originated films by Coleman and Thomas[12] agrees with similar analyses by Grigorovici and Mănăilă[13] and by Richter and Breitling[14,22] on evaporated films and our x-ray patterns on sputtered films. Thus we have the unresolved puzzle of why the silane-originated films apparently have the same structural properties as evaporated or sputtered amorphous Si, but different electrical and optical properties. The differences may be spurious, e.g., hydrogen contamination remaining from the silane. It is interesting to note that Chittick *et al.*[4] report that annealing raises the conductivity rather than lowers it, as observed in evaporated and sputtered films. This may be due to the driving off of hydrogen, leaving behind a Si film more like the evaporated or sputtered variety. If the difference is not spurious, then one must look for structural variations in more detail than can be seen with x rays. We suggest ESR as one tool that should be useful in this respect.

In order to compare the properties of amorphous Si with other amorphous semiconductors, we must recall not only the distinction made in the introduction between latticelike and liquidlike amorphous structures, but also the further restriction imposed by the hypothesis of a microstructural model. We must realize that it may not be appropriate to look for similarities between amorphous Si and the glassy semiconductors such as the much studied chalcogenides.[18,33,34] Thus, in the above discussion of amorphous Si, we have consciously refrained from using the models that Mott,[36] Gubanov,[19] Cohen *et al.*,[37] and others have proposed for disordered electronic systems.

The amorphous semiconductors most comparable to Si are Ge and SiC. Both of the materials have been prepared as amorphous films either by evaporation or sputtering. As has already been mentioned, the electrical conductivities of Ge[5] are of the same magnitude and follow the same annealing trends as Si. Mogab and Kingery[6] report similar results on SiC. The ESR of all three of these amorphous semiconductors[16] has been found to be similar to the surface resonances of the corresponding crystalline forms. In this laboratory we have observed that the optical-absorption constants of amorphous Ge and SiC decrease with annealing in a similar way as for amorphous Si. An important exception to the self-consistency of the optical results is the sharp absorption edge of amorphous Ge reported by Donovan, Spicer, and Bennett[7] occurring at nearly the same energy as the single-crystal Ge edge. Others[1,8,9,52] have reported an exponential tail on the leading edge of the fundamental optical-absorption spectrum of amorphous Ge, which Donovan *et al.*[7] do not see in their very careful measurements. We observe a tail, although not as clearly exponential as in Ge, in the optical-absorption spectrum of amorphous Si. In terms of the microstructural model, the answer may lie in the different thicknesses and growth conditions of amorphous Ge. For example, the amorphous Ge crystallization temperature[14,22,42] is considerably lower and therefore closer to room temperature than either the Si or SiC crystallization temperatures. Therefore, Ge is a poor choice for stable films near room temperature because during deposition there is the possibility of heating the film enough for some crystallization to occur.[42] Glass[8] has shown that the exponential tailing in polycrystalline Ge films is a strong function of growth temperature. In preliminary experiments we have also observed substrate and film-thickness dependences of the absorption spectrum of sputtered amorphous Ge. Furthermore, both crystal and amorphous Ge have strong optical absorptions in the same spectral region. Therefore it is more difficult to extract the effect of disorder than in the case of Si with only a weak indirect transition in the region of interest.

[52] J. Tauc, A. Abraham, R. Zallen, and M. Slade, in Proceedings of the International Conference on Amorphous and Liquid Semiconductors, Cambridge, 1969 (unpublished).

V. SUMMARY

We have examined the x-ray diffraction, ESR, near-infrared and visible optical-absorption spectra, and electrical conductivity of amorphous Si films and found that all of the results, except the lack of long-range order, depend on the thermal history of the samples. A building-block model with structures in the 10 to 15 Å range is suggested as an interpretation of the x-ray, ESR, and conductivity results. The tails in the optical-absorption spectra are attributed to local strains and fields associated with the microstructural surfaces. The relatively large fundamental absorption of amorphous Si compared to the crystalline state implies a breakdown of the crystal-momentum selection rule of large shifts of crystal band energies. According to the model, the low electrical conductivity and its further decrease upon annealing is due to barriers between building blocks. While the evidence presented for the microstructural point of view is not overwhelming, it is stronger than the evidence for the alternative model of a continuous network.

ACKNOWLEDGMENTS

We acknowledge the technical assistance of L. Buszko, W. Fitzpatrick, J. Angillelo, and J. Keller. We thank J. Cuomo for providing the SiC and silane-decomposed Si samples. Dr. W. Howard, Dr. M. I. Nathan, Dr. F. Stern, and Dr. T. B. Light have provided stimulating discussions and useful critical comments.